Minimal model for complex dynamics in cellular processes

C. Suguna, Kanchan K. Chowdhury, and Somdatta Sinha*
Centre for Cellular and Molecular Biology, Hyderabad 500 007, India
(Received 11 June 1999)

Cellular functions are controlled and coordinated by the complex circuitry of biochemical pathways regulated by genetic and metabolic feedback processes. This paper aims to show, with the help of a minimal model of a regulated biochemical pathway, that the common nonlinearities and control structures present in biomolecular interactions are capable of eliciting a variety of functional dynamics, such as homeostasis, periodic, complex, and chaotic oscillations, including transients, that are observed in various cellular processes.
[S1063-651X(99)14911-0]

PACS number(s): 87.80.Vt, 05.45.−a

I. INTRODUCTION

Biochemical reactions underlie cellular functions. The variety of functional dynamics is a consequence of the nonlinearities inherent in multiple modes of biochemical regulation, such as cooperativity and kinetics at the levels of gene expression, protein synthesis, enzyme activity, receptor function, and transport processes. These highly networked reactions utilize single, multiple, and coupled negative and positive feedback processes as the primary mode of regulation to coordinate and control the accumulation of intermediates and end product of the pathway [1–4]. Of the two types of feedback, the negative feedback processes desensitize the system to perturbations, such as environmental or developmental noise. They have a stabilizing role and help in conservation of energy in cellular economy, and are, therefore, naturally selected to be the most common form of regulation in pathways. Though potentially destabilizing, many biochemical processes employ positive feedback for excitable dynamics and for the amplification needed in switching and rapid-response processes [5,6]. Homeostasis has been considered as the most common type of dynamics in biology, but it is becoming increasingly evident that multistable, multirhythmic, oscillatory, chaotic, and transient processes are more generic and ubiquitous at various levels of organization of biological systems having important functional consequences [7–9].

For example, along with sustained oscillations, which were observed many years ago [10], other types of dynamics, such as multiple stable states, birhythmicity, and complex oscillations have also been reported subsequently in glycolysis of cell-free extracts of yeast cells [11,12]. Similar diversity in dynamics has been found in many other biochemical reactions under a variety of experimental conditions—the peroxidase-oxidase reactions and hormone oscillations [13–19], cyclic Adenosine Mono-Phosphate (cAMP) oscillations in cellular slime mold *dictyostelium discoideum* [20], glycolysis and insulin secretion in pancreatic beta cells [9,21,22], neuronal systems [23], and calcium oscillations of different frequency and amplitude [24–28]. Recently, dynamic phenomena of another type are attracting wide attention due to their interesting signaling role in diverse cellular processes. These are the transient processes, e.g., ''sparks'' and ''puffs'' in calcium oscillations, and spatial waves in many cell types [29,30].

One interesting aspect of these phenomena is the emergence of the multiplicity of roles of the same product whose different dynamics signal different cellular functions—including cell death [28,30]. This requires the underlying controls of the pathway to be flexible, yet precisely regulated, to yield output signals of the required dynamics. Thus for optimal performance, requiring stability, sensitivity, and multiplicity of dynamics, a combination of negative and positive feedback processes is useful. In reality, the biochemical details of the pathways are generally quite diverse, elaborate, and involve complex regulatory controls. But a minimal regulatory structure in a complicated pathway may be sufficient to give rise to the required functional dynamics—the additional complexities being the outcome of evolutionary selection for robustness and redundancy. The aim of this paper is, thus, to see if a skeletal pathway, incorporating the minimal combination of a pair of coupled negative and positive feedback processes, representing the stability and sensitivity properties of the system, can exhibit a multitude of dynamics, as observed in real biochemical reaction pathways.

As the minimal model we consider a three-variable pathway comprised of only two feedback loops—one negative and one positive in the form of common cellular control processes in cells—and enumerate the variety of dynamics that this pathway can exhibit for changes in its parameters. We show that this simple model pathway not only exhibits equilibrium and periodic dynamics, but also shows birhythmicity, complex oscillations, chaos, and other complexities, such as fractal basin boundaries that give rise to interesting transient dynamics under noise. Thus, even at this elementary level, the pathway possesses a wide range of functional diversity that is observed in complex biochemical pathways with more elaborate controls. It would, therefore, be useful to delineate the important control structures for manipulation and modification in diseased or engineered biochemical pathways.

II. MINIMAL PATHWAY AND METHODS

The model biochemical pathway is a three-step reaction sequence (Fig. 1) where the substrate S1 is converted to S2,

*Electronic address: sinha@ccmb.ap.nic.in

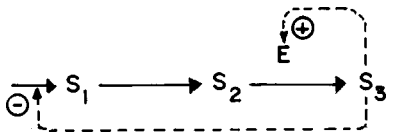

FIG. 1. The minimal biochemical pathway: a three step reaction sequence with inhibition of S1 by endproduct S3 and activation of the allosteric enzyme E by S3.

which then is converted to the product S3 through an enzyme (E)-mediated reaction. There are two levels of control built into this linear chemical reaction through two feedback loops—end-product inhibition of S1 by S3 (a negative feedback) and the autocatalytic production of S3 from S2 by the enzyme E (a positive feedback). For the feedback processes we consider common molecular interactions that are abundantly employed in the biochemical pathways in cells. We assume that the S3-S1 interaction for end-product inhibition follows cooperative kinetics [31], and the autocatalytic production of S3 is through the allosteric property of the enzyme E [32]. These are nonlinear kinetic processes that are common in mechanisms of biochemical regulation and are widespread in both genetic and metabolic reactions underlying cellular processes, such as the cell cycle, gene repression/induction, glycolysis, hormonal signaling, cAMP oscillations in cellular slime molds, calcium-induced-calcium-release (CICR), etc. [9,31,34]. Thus we consider this to be a simple and general scheme that may represent a large variety of functional dynamics observed in cellular systems.

The time evolution of this model pathway can be described by the following equations:

$$\frac{dx}{dt} = F(z) - kx,$$

$$\frac{dy}{dt} = x - G(y,z),$$

$$\frac{dz}{dt} = G(y,z) - qz, \tag{1}$$

where x, y, and z are the normalized concentrations of the substrates S1, S2, and S3, and k and q are parameters controlling the rates of degradation of S1 and S3 that follow first order kinetics and are nonsaturated. The nonlinear functions $F(z)$ and $G(y,z)$ represent the negative and positive feedback terms, respectively. $F(z)$ is a function of the end product alone and the reaction requires cooperative binding of n molecules of z for inhibition. The positive feedback term $G(y,z)$ involves the allosteric enzyme E that obeys the concerted transition model [32]. E follows the quasi-steady-state hypothesis for the enzymatic forms and is considered to be a dimer with exclusive binding to the more active conformational state [33]. These two regulatory processes in Eq. (1) can be written as

$$F(z) = \frac{1}{1+z^n}, \tag{2}$$

$$G(y,z) = \frac{Ty(1+y)(1+z)^2}{L+(1+y)^2(1+z)^2}, \tag{3}$$

where T and L are maximum velocity and allosteric constant of the enzyme E. Thus this simple three-step regulated reaction sequence shown in Fig. 1 and described by Eqs. (1), (2), and (3) is our minimal model.

This model reaction system has been studied using a combination of analytical and numerical methods. The basal parameter values for this pathway were based on typical experimental values available for other cellular processes possessing similar positive and negative feedback mechanisms [33–36], and have been chosen as $n=4$, $L=10^6$, $T=10$, $k=1$, $q=0.01$. All parameters and variables are dimensionless here. Numerical simulations have been done for a range around these basal values. The system of equations yields only one positive real steady state for a large range of parameter values. The local stability of this steady state has been analyzed using linear stability analysis. The dynamical behaviors of x, y, and z have been numerically simulated using Mathematica ver 2.2.

III. RESULTS AND DISCUSSION

We describe the nature and role of the common control properties and the variety of dynamics exhibited by our minimal pathway upon variation of parameters.

A. Nature of the regulatory feedback processes

Figure 2 summarizes the response of the two feedback controls—end-product inhibition (negative feedback) $F(z)$ and allosteric activation (positive feedback) $G(y,z)$ to changing substrate concentrations. The negative feedback term $F(z)$ [see Eq. (2)] is a function of the end product alone and Fig. 2(A) shows the extent of feedback inhibition with increasing z for different values of the cooperativity of inhibition n. With increasing z, $F(z)$ decreases sharply, and at higher values of n this effect becomes stronger, making the rate of synthesis of S1 negligible for large concentrations of the end product. Thus, at higher values of n (3 or 4 here), $F(z)$ acts like a switch that shuts off or drastically reduces the synthesis of x beyond a small value of z. It is clear that with increasing cooperativity (n) the negative feedback control becomes tighter as compared to when there is no cooperativity ($n=1$). The positive feedback process modeled by $G(y,z)$ [see Eq. (3)] involves the autocatalytic synthesis of S3 from S2, aided by the allosteric enzyme E, and is, therefore, a function of both y and z. As shown in Fig. 2(B), $G(y,z)$ has a sigmoidal saturation curve for increasing concentrations of both the substrates y and z. Increasing z requires reduced y for ensuring the same amount of positive feedback control to occur. Thus the allosteric transition from a low-activity, low-affinity conformation to a high-activity, high-affinity one is promoted by either y or z, and the transition is steeper at higher concentrations of the two substrates.

B. Stability and dynamics

It is clear that the two feedback terms respond in an opposite manner for a small increase in the end product z. The final functional response (dynamics) of the pathway, given the nature of the two opposing regulatory processes, would depend much on the other processes, such as the removal/

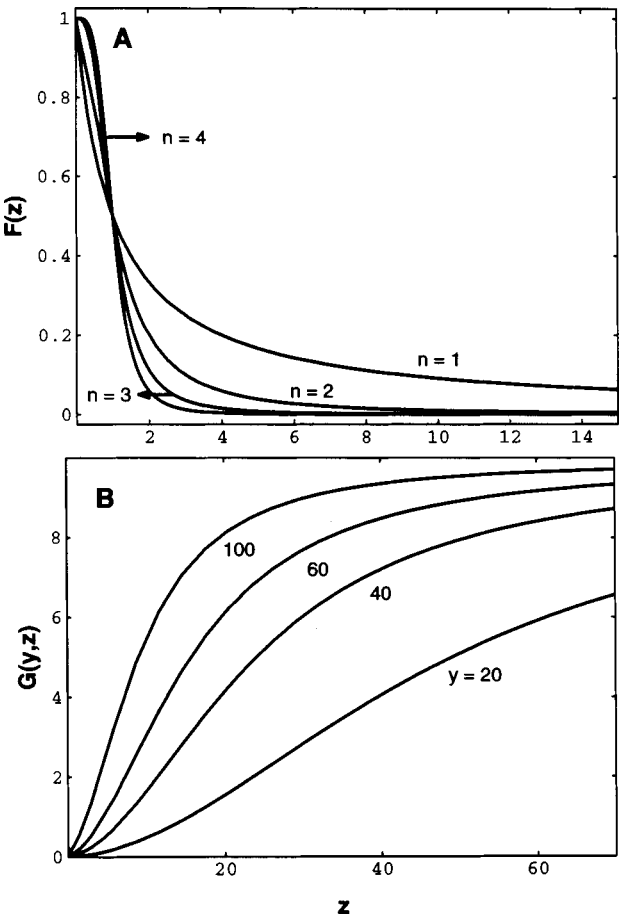

FIG. 2. Nonlinear feedback regulation: (A) Feedback inhibition, $F(z)$ with increasing concentration of the end product (z) for different values of cooperativity (n); (B) feedback activation, $G(y,z)$, as a function of the end product (z) for different concentrations of y.

degradation rates of the substrate S1 and end product S3 (k and q, respectively), which increase or decrease the flux of material through the pathway. In Figs. 3(A)–3(D), we show the (k,q) parameter space describing the stability regions where the pathway shows equilibrium and oscillatory (simple and complex) dynamics for different values of the cooperativity of the negative feedback (n).

There are three regions in each plot—the region marked with crosses represents (k,q) values where the steady state is negative and hence not of interest here; the dotted region is where the steady state is a fixed point, and the pathway returns to the equilibrium state on perturbation; and the blank closed region is where the steady state is unstable (through local linear stability analysis). Generally, the pathway shows equilibrium dynamics both for very low and high rates of degradation of S1 and S3, but as the cooperativity of the negative feedback (n) increases, the isolated region showing unstable dynamics increases, and it is the largest for $n=4$. To study the dynamics within the unstable region, we simulated the model equations for $q=0.1$ for a range of k values. The results are shown in Fig. 3(E) for $n=1$ to 4. For low cooperativity ($n=1,2$), the pathway only shows simple periodic dynamics in this range of k values. But for $n>2$, a whole range of complex behavior, such as period-doubling bifurcations, chaos, complex oscillations, etc., occur along with simple limit cycle dynamics. This region of complex dynamics is the largest for $n=4$, while the pathway shows simple limit cycle oscillations for basal values of k and q ($k=1$, $q=0.01$). This indicates that, even if the normal dynamics is periodic, any small changes in k can induce complex behavior in the pathway functioning, enabling it to exhibit multiplicity in dynamics. We studied this region in greater detail.

Figures 4(A)–4(H) show the (y,z) phase plots depicting the variety of unstable dynamics exhibited by this minimal pathway for $q=0.1$ and $n=4$, with increasing k. Within this unstable region, the pathway starts and ends with simple limit cycle oscillations with much complexity in dynamic behavior for the intervening k values. Figure 4(A) shows simple oscillatory behavior (limit cycle with amplitude ~ 30 and time period ~ 80) for $k=0.0023$, which is stable against small perturbations in substrate concentrations. We designate this limit cycle as the ''type I'' attractor. For a very small increase in k, at $k=0.0024$, the dynamics changes significantly. Depending on the initial conditions, the pathway evolves to two different types of attractors—the period-doubled type I attractor and another large attractor (''type II'') with eight times higher time period and almost twice the amplitude of the type I attractor. Both these attractors are plotted together in Fig. 4(B) for the convenience of comparison. For small increases in k, the two attractors continue to coexist and the type I attractor goes through further bifurcations [Fig. 4(C), for $k=0.002\,75$], which separate into bands [Fig. 4(D), for $k=0.0028$]. The two chaotic bands then spread until they merge and one gets chaotic oscillations where large complex oscillations (bifurcated type II attractor) are interspersed with small high frequency random oscillations (chaotic type I attractor) shown in Fig. 4(E) for $k=0.003$. A similar sequence of dynamics was also observed in the Brusselator model, but only on periodic forcing [37].

The complexity in pathway dynamics changes at higher values of k. The high frequency type I attractor disappears and the pathway goes through a series of changes in dynamics of the type II attractor only. Here the dynamics is robust against small perturbations in substrate concentrations. There also exist periodic windows in this range of k [Fig. 4(F) for $k=0.006$], period reversals [Fig. 4(G) for $k=0.009$], complex oscillations, asymmetric bifurcation [38] giving rise to the ''kink'' in the type II attractor, etc. With increasing k, the time period of the type II limit cycle reduces, eventually showing a robust, simple, periodic behavior [Fig. 4(H), for $k=0.028$] again, with an amplitude of almost twice that at $k=0.0023$ [Fig. 4(A)] but of similar time period, thus completing a full cycle of behavioral modes. Thus the functional dynamics exhibited by this simple pathway is quite complex and sensitive to kinetic parameters and substrate concentrations.

C. Coexistence of attractors and their basins of attraction

The coexistence of two different attractors, as shown in Figs. 4(B)–4(E), indicates that this biochemical pathway is capable of functioning in two different types of oscillatory modes under experimental conditions, even when all parameters are the same. Figure 5(A) shows these two time series of the end product z plotted together to show clearly that the type II attractor has a larger amplitude and higher time pe-

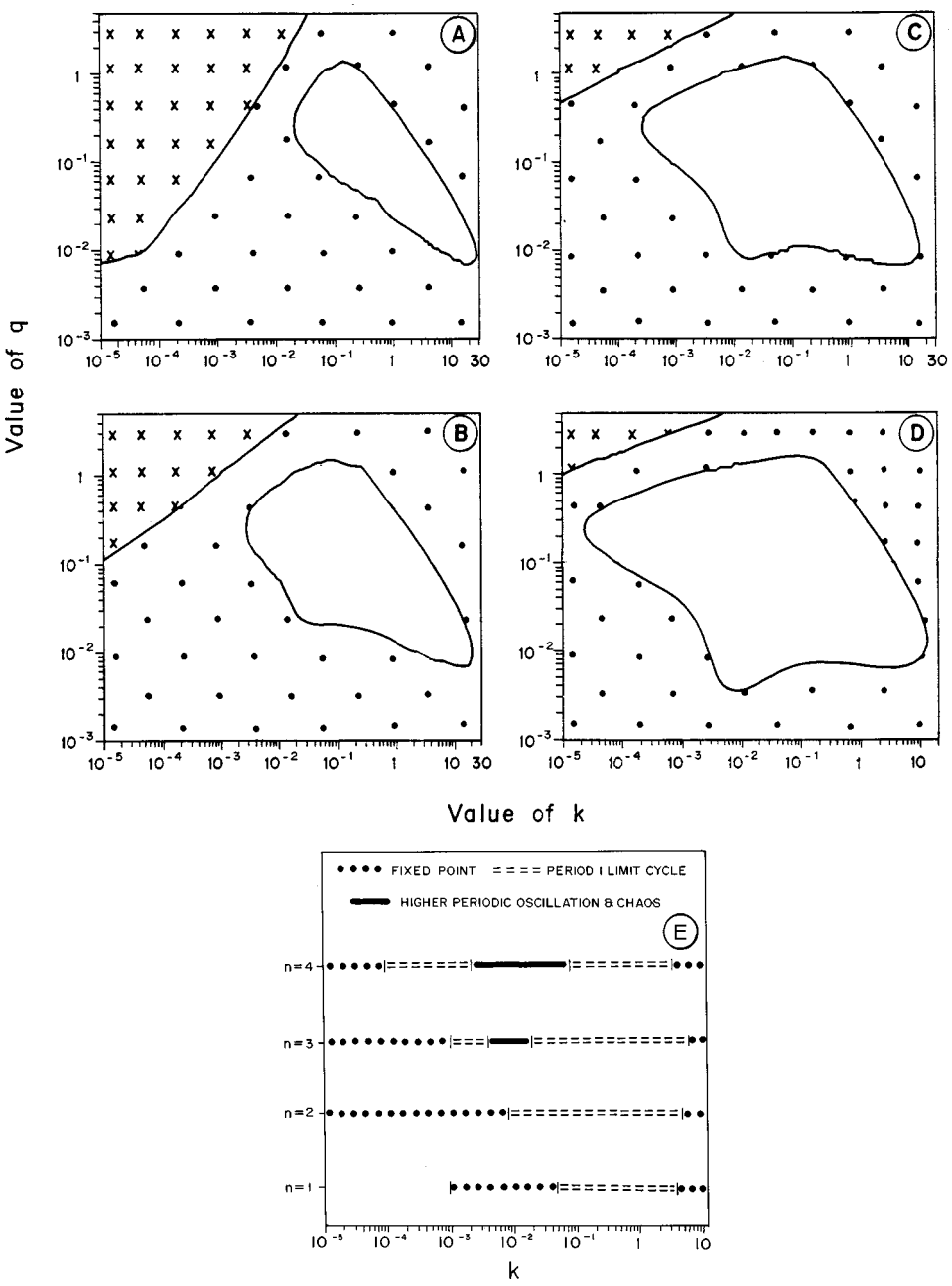

FIG. 3. Stability plots in (k,q) parameter space for different values of the cooperativity (n). The $\times$ denotes negative steady states, $\bullet$ denotes equilibrium dynamics, and the blank region denotes (k,q) values at which the steady state is unstable for (A) $n=1$, (B) $n=2$, (C) $n=3$, and (D) $n=4$. (E) Dynamics at different values of n, for variation of k, with $q=0.1$. All other parameters are kept at their basal value.

riod. Figure 5(B) shows the relative positions of the two attractors in the three dimensional (x,y,z) phase space. The type I attractor is almost two dimensional because its spread in the x direction is very small. It is clear from the figure that the phase space of the two attractors overlaps considerably, thereby raising interesting questions about the predictability of the final dynamical state of the pathway on perturbation (final state sensitivity).

We looked for the basins of attraction of the two coexisting attractors by undertaking a thorough search of the (y,z) phase space near the positive steady state. The equations describing the model biochemical pathway were simulated for a range of initial y,z values around the steady state at different scales, and the type of the asymptotic attractor was noted. It was observed that the pathway evolved to either one of the attractors, depending on initial conditions. Figures 6(A)–6(C) show the mappings (in the y,z plane) of their basins of attraction (crosses for the type I and dots for the type II attractor) at three different progressively finer scales. The figure shows that, not only is the evolution to the final state unpredictable, there are no clearly defined boundaries in the phase space for the two attractors at any scale. Also, there is self-similarity revealing a fractal nature of the basin of attraction of these nonchaotic attractors. The implications of this type of behavior in biological processes can be very interesting and important from the functional point of view.

D. Characterization of the chaotic attractor

It is clear that the common and biologically realistic nonlinearities used in this minimal pathway can give rise to very complex dynamics. Figure 4 shows that the small-amplitude, high frequency type I attractor goes through period-doubling bifurcations, and the coexisting, large, type II attractor goes through bifurcations and complex shape changes in the phase space. Because of the fractal nature of the basins of attraction

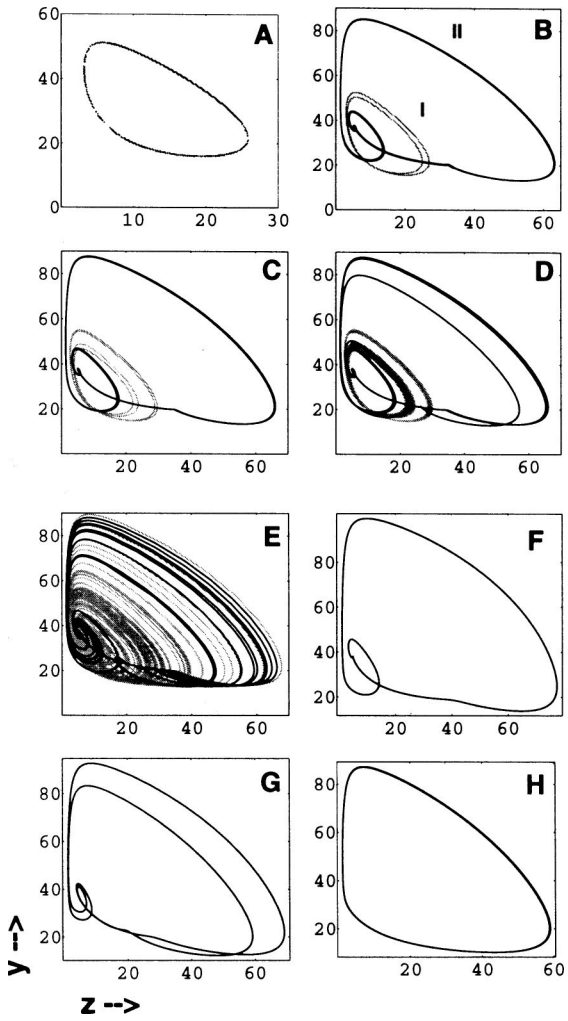

FIG. 4. Phase plots for different dynamical behaviors of the end product (z) for increasing values of k at $q=0.1$. (A) Type I attractor for $k=0.0023$. (B) Coexistence of bifurcated type I attractor (marked I) and type II attractor (marked II) for $k=0.0024$. (C) Coexistence of period 4, type I attractor and type II attractor for $k=0.002\,75$. (D) Type I attractor bifurcated into two chaotic bands with coexisting type II attractor for $k=0.0028$. (E) Chaotic type I and complex type II attractors for $k=0.003$. (F) Type II attractor for $k=0.006$ (periodic window). (G) Type II attractor for $k=0.009$ (period reversal). (H) Limit cycle for $k=0.028$.

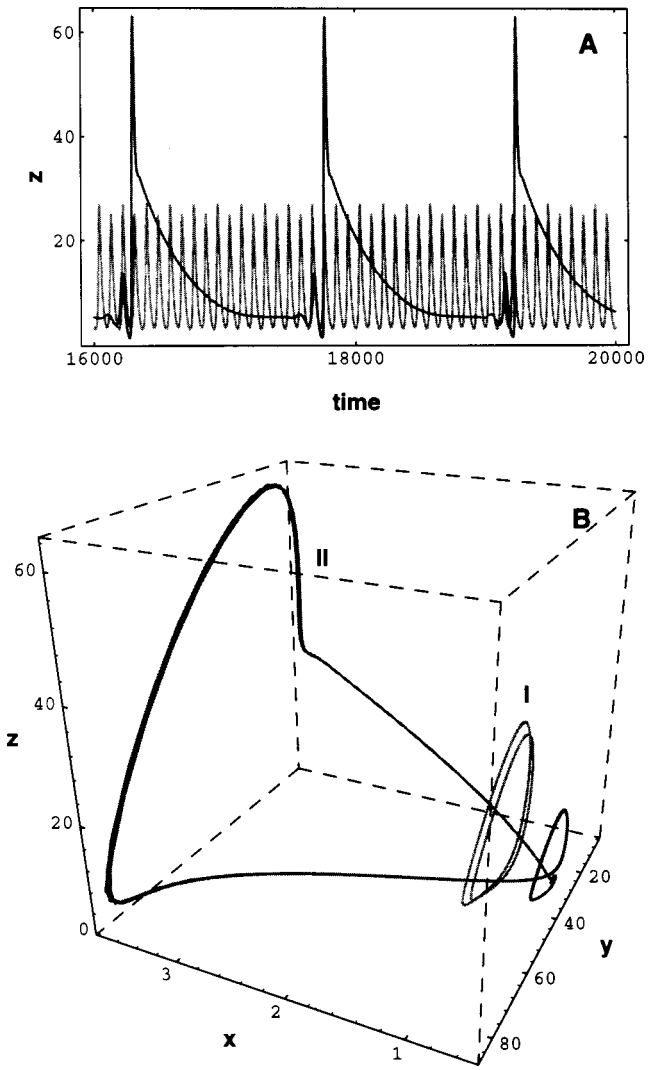

FIG. 5. Birhythmicity for $k=0.0024$, $q=0.1$, and $n=4$. (A) Asymptotic temporal behavior of z. Both type I and type II attractors are plotted together for comparison. (B) Three dimensional phase plots of the two attractors (type I and type II).

of these two attractors, the time evolution of the pathway is seen to have very long stretches of chaotic type I oscillations interspersed with regions of large-amplitude complex type II oscillations. We attempted to describe this complexity in the dynamics by seeking a simpler representation of the system by deriving a one-dimensional map from the model. Such a representation simplifies the geometric description of the system by reducing the number of state space variables, but still contains the essential information about the behavior [39–41].

From the relative positions of the two attractors in Fig. 5(B), one can see that the type I attractor is trapped in an almost two-dimensional sheet of the phase space. The steady state, which is situated near the kink of the larger attractor, is a saddle point of index 2. Figures 7(A) and 7(B) show the time series of the end product z and the chaotic type I attractor in the (y,z) phase plane for $k=0.0029$. Since the system is highly dissipative and the three-dimensional (3D) trajectories rapidly converge to a nearly 2D sheet on which they remain trapped, the correlation dimension [42,43], of this attractor, was found to be 1.65. We constructed a Poincaré section [41] along line PQ for the chaotic attractor in Fig. 7(B), in a plane perpendicular to the (y,z) plane. The one-dimensional return map constructed from this is shown in Fig. 7(C). The points fall along a smooth one-dimensional curve with a single maximum, along with an additional branch. This kind of a situation has been found experimentally as well as theoretically in other systems, such as the Belousov-Zhabotinsky reaction [44], peroxidase-oxidase reaction [14], and diode circuit reaction [41], and is indicative of higher order dynamics. The slope of the hump at the fixed point is found to be -1.75, which is clearly indicative of period-doubling bifurcations and chaos.

IV. CONCLUSIONS

The biochemical pathways underlying the variety of cellular processes are generally quite elaborate and involve multiple regulatory controls connecting many reaction branches.

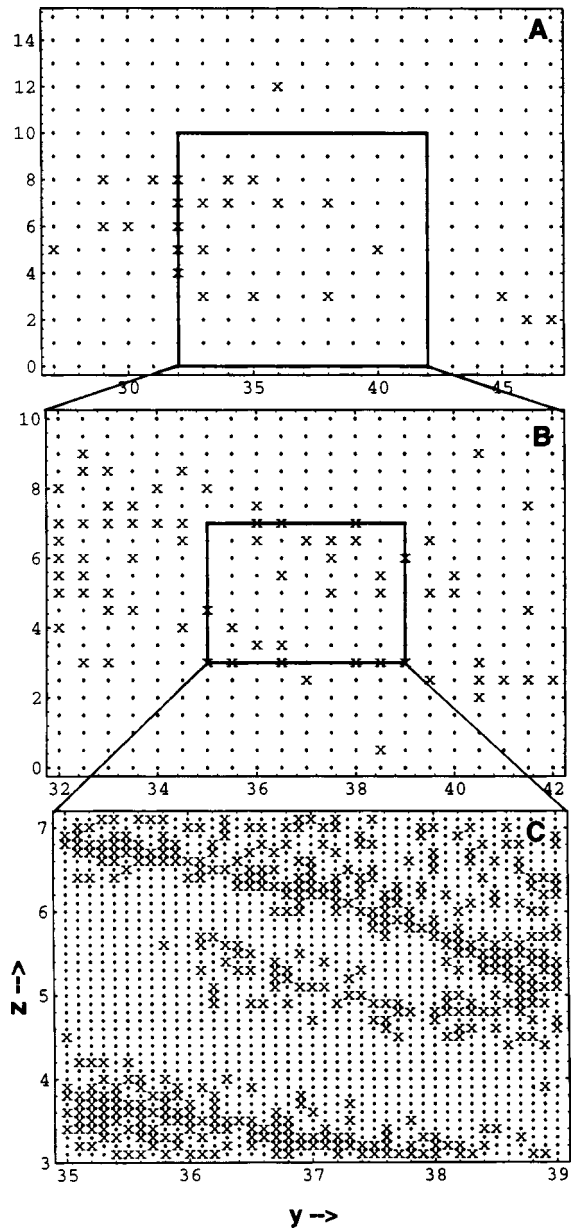

FIG. 6. Basins of attraction of the two attractors (x for type I and • for type II) for different initial conditions in the (y,z) plane with x fixed at the steady-state value for $k=0.0024$, $q=0.1$. (B) and (C) are magnifications of the boxed regions in (A) and (B), respectively. Transients of about 6000 time units are discarded in the simulation for each initial condition.

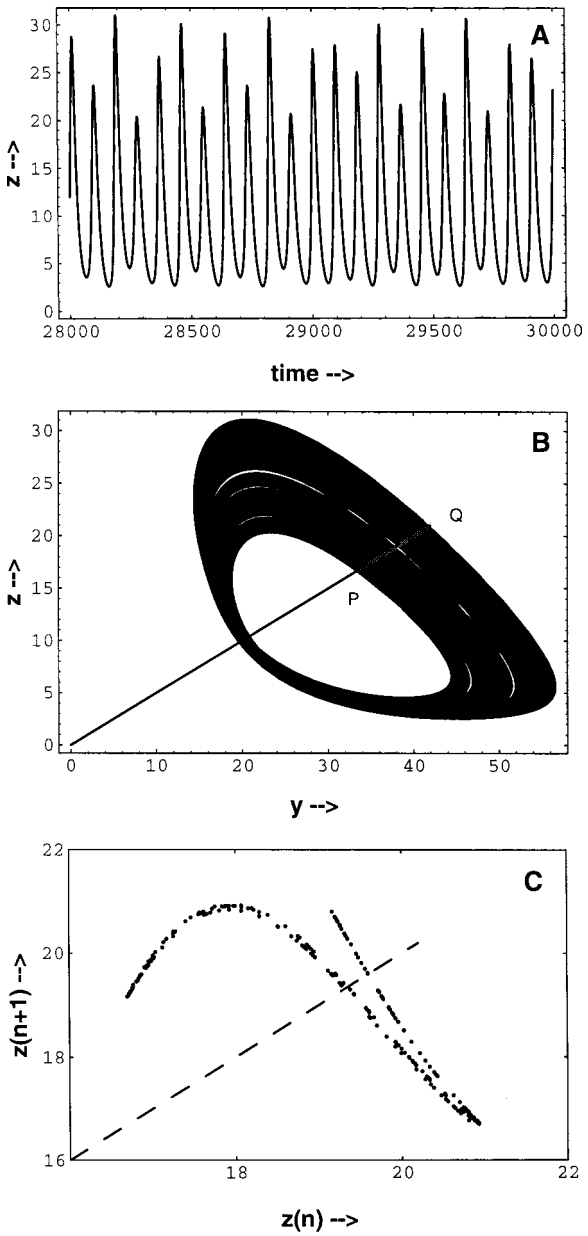

FIG. 7. Characterization of the chaotic attractor at $k=0.0029$, $q=0.1$. (A) Time series of z after removing transients. (B) Phase plot in the (y,z) plane with Poincaré section along line PQ, parallel to x plane. (C) One dimensional return map of the attractor. The slope of the map at the equilibrium point is -1.75.

The experimentalist aims to delineate the details of each in molecular terms. The cell employs few types of kinetic regulatory mechanisms that impart common features in apparently diverse/dissimilar processes. The aim of this study is to explore the minimal regulatory structure that can give rise to the variety of functional dynamics observed in diverse cellular processes, presuming that the additional complexities are the outcome of evolutionary selection primarily for robustness, redundancy, and network connectivity, which have important adaptive roles.

We have shown that a minimal model, incorporating common regulatory processes, is capable of showing a diverse variety of dynamical behaviors—from equilibrium to oscillatory, complex, chaotic, and transients—that are exhibited by many cellular processes in cells/tissues. This capability of having diverse dynamics for different parameters and conditions enables cells to utilize common resources for vastly differing functions. For instance, calcium signals are used by cells to trigger cellular functions ranging from fertilization, development, and differentiation, to death [30]. The same calcium signals regulate cardiac, muscular, and neuronal activities by using different combinations of spatial and temporal controls. The response of the cell is optimized by the frequency and level of the oscillatory calcium—termed as frequency and amplitude coding [28,30]. In order to achieve such versatility the biochemical reaction pathway involved should be flexible yet precisely regulated to yield molecular signals with differing periodicity, or the same periodicity but differing amplitudes, with variation in pathway parameters

or substrate concentrations. We have shown that this minimal pathway can achieve such versatility. The existence of birhythmicity and the fractal basins of attraction facilitate the process of transient signaling (spontaneous or activated) under the omnipresent experimental noise in biological systems, as observed in spontaneous events, such as calcium ''sparks'' or ''puffs'' [45]. Such mechanisms may also underlie random switching between alternative regulatory paths in cells [46]. Though we have considered spatial homogeneity in our model, these transients in cells in the tissue can give rise to spatial waves as observed in many systems [29,30]. A decrease in time period of oscillations with increasing parameter shown by this minimal pathway is also observed in young mice for circadian rhythms showing age-dependent reduction in the time period of the rhythm [47].

The functional diversity exhibited by this minimal pathway is indicative of the possibility of greater diversity in the complex and realistic pathway. An understanding of this system can, on the one hand, yield much unification in the source of diverse cellular phenomena and, on the other, lead to a better understanding of the more complex biochemical reaction networks controlling cellular functions, so that one can design necessary controls for the required behavior, devise methods to correct altered dynamics [48,49], or engineer new pathways with the required dynamical behavior.

ACKNOWLEDGMENT

The authors thank the Bioinformatics Centre, CCMB, for providing the software package.

[1] A. Cornish-Bowden, *Fundamentals of Enzyme Kinetics* (Butterworths, London, 1979).
[2] M. Ptashne, *A Genetic Switch. Gene Control and Phage* λ (Cell Press, Cambridge, MA, and Blackwell Scientific, Palo Alto, CA, 1986).
[3] M. A. Savageau, *Biochemical Systems Analysis. A Study of Function and Design in Molecular Biology* (Addison-Wesley, Reading, MA, 1976).
[4] J. J. Tyson and H. G. Othmer, Prog. Theor. Biol. **5**, 1 (1978).
[5] D. E. Koshland, Jr., A. Goldbeter, and J. B. Stock, Science **217**, 220 (1982).
[6] J. E. Lisman and J. R. Fallon, Science **283**, 339 (1999).
[7] L. Glass and M. C. Mackey, *From Clocks to Chaos. The Rhythms of Life* (Princeton University Press, Princeton, NJ, 1988).
[8] A. T. Winfree, *The Geometry of Biological Time*, Biomathematics Vol. 8 (Springer-Verlag, New York, 1980).
[9] A. Goldbeter, *Biochemical Oscillations and Cellular Rhythms* (Cambridge University Press, Cambridge, UK, 1996).
[10] A. K. Ghosh and B. Chance, Biochem. Biophys. Res. Commun. **16**, 174 (1964).
[11] M. Markus, D. Kuschmitz, and B. Hess, FEBS Lett. **172**, 235 (1984).
[12] K. Nielsen, P. G. Sorensen, F. Hynne, and H.-G. Busse, Biophys. Chem. **72**, 49 (1998).
[13] T. Hauck and F. W. Schneider, J. Phys. Chem. **97**, 391 (1993).
[14] A. C. Moller, M. J. B. Hauser, and L. F. Olsen, Biophys. Chem. **72**, 63 (1998).
[15] S. Nakamura, K. Yokota, and I. Yamazaki, Nature (London) **222**, 794 (1969).
[16] L. F. Olsen and H. Degn, Nature (London) **267**, 177 (1977).
[17] M. S. Samples, Y.-F. Hung, and J. Ross, J. Phys. Chem. **96**, 7338 (1992).
[18] K. R. Valeur and L. F. Olsen, Biochim. Biophys. Acta **1289**, 377 (1996).
[19] I. Yamazaki and K. Yokota, Mol. Cell. Biochem. **2**, 39 (1973).
[20] G. Gerisch and B. Hess, Proc. Natl. Acad. Sci. USA **71**, 2118 (1974).
[21] H.-F. Chou, N. Berman, and E. Ipp, Am. J. Physiol. **262**, E800 (1992).
[22] B. A. Cunningham, J. T. Deeney, C. R. Bliss, B. E. Corkey, and K. Tornheim, Am. J. Physiol. **271**, E702 (1996).
[23] U. S. Bhalla and R. Iyengar, Science **283**, 381 (1999).
[24] M. J. Berridge, P. H. Cobbold, and K. S. R. Cutbertson, Philos. Trans. R. Soc. London, Ser. B **320**, 325 (1988).
[25] C. C. Canavier, D. A. Baxter, J. W. Clark, and J. H. Byrne, J. Neurophysiol. **69**, 2252 (1993).
[26] J. Hounsgaard, H. Hultborn, B. Jesperson, and O. Kiehn, J. Physiol. (London) **405**, 345 (1988).
[27] A. Malgaroli and J. Meldolesi, FEBS Lett. **283**, 169 (1991).
[28] G. Dupont and A. Goldbeter, BioEssays **20**, 607 (1998).
[29] H. Cheng, W. J. Lederer, and M. B. Cannel, Nature (London) **262**, 740 (1993).
[30] M. J. Berridge, M. D. Bootman, and P. Lipp, Nature (London) **395**, 645 (1998).
[31] L. A. Segel, *Mathematical Models in Molecular and Cellular Biology* (Cambridge University Press, Cambridge, UK, 1980).
[32] J. Monod, J. Wyman, and J. P. Changeaux, J. Mol. Biol. **12**, 88 (1965).
[33] A. Goldbeter and G. Nicolis, Prog. Theor. Biol. **4**, 65 (1976).
[34] B. C. Goodwin, *Analytical Physiology of Cell and Developing Organisms* (Academic Press, London, 1976).
[35] S. Sinha and R. Ramaswamy, BioSystems **20**, 341 (1987).
[36] J. J. Tyson, J. Theor. Biol. **103**, 313 (1983).
[37] B.-L. Hao and S. Zhang, J. Stat. Phys. **28**, 769 (1982).
[38] D. R. Moore, J. Toomre, E. Knobloch, and N. O. Weiss, Nature (London) **303**, 663 (1983).
[39] O. Decroly and A. Goldbeter, J. Theor. Biol. **113**, 649 (1985).
[40] J. D. Farmer, E. Ott, and J. A. Yorke, Physica D **7**, 153 (1983).
[41] R. C. Hilborn, *Chaos and Nonlinear Dynamics* (Oxford University Press, Oxford, UK, 1994).
[42] P. S. Addison, *Fractals and Chaos. An Illustrated Course* (Institute of Physics Publishing, Bristol, UK, 1997).
[43] P. Grassberger and I. Procacia, Phys. Rev. Lett. **50**, 346 (1983).
[44] J. C. Roux, R. H. Simoyi, and H. L. Swinney, Physica D **8**, 257 (1983).
[45] M. B. Cannel and C. Soeller, Trends Pharmacol. Sci. **19**, 16 (1998).
[46] H. H. McAdams and A. Arkin, Trends Genet. **15**, 65 (1999).
[47] V. K. Sharma and M. K. Chandrasekaran, J. Exp. Zool. **280**, 321 (1998).
[48] S. Parthasarathy and S. Sinha, Phys. Rev. E **51**, 6239 (1995).
[49] N. Parekh, S. Parthasarathy, and S. Sinha, Phys. Rev. Lett. **81**, 1401 (1998).